On Nonlinear Evolutions of the Intense, Short Laser Pulse in the Under-Dense Plasma

Jam Yazdanpanah[1,a)], Elnaz Yazdani[2], Elnaz Khalilzadeh[1] and Amir Chakhmachi[1]

[1]*The Plasma Physics and Fusion Research School, Tehran, Iran*

[2]*Laser and Optics Research School, Tehran, Iran*

a) Electronic mail: jamyazdan@gmail.com

ABSTRACT

Nonlinear evolutions of an ultra-intense, short laser pulse due to the wake excitation inside the plasma are studied by means of detailed Particle-In-Cell (PIC) simulations and comprehensive analyses. Pulse lengths both longer and shorter than the plasma wavelength are considered. It is turned out that the system shows adiabatic behavior as long as the plasma evolves very slowly in the Pulse Co-Moving (PCM) frame due to the ignorable radiation back-reactions. A sophisticated treatment of the adiabatic regime is presented, based on the proper application of the local conservation laws in the PCM frame in conjunction with the Lorentz transformations. In this context, equations for the overall pulse evolutions are reduced into a single equation in terms of the global pulse group-velocity. Due to the proven equality between the local phase velocities of the plasma wave and the radiation, anomalies are observed in this regime, in the global

group velocity and the plasma dispersion. The group velocity shows non-explicit density dependency and of remaining above the linear value over a long period of the propagation. These results are successfully examined against PIC simulations and their consistency with the other system evolutions and the physical intuition is fully discussed. Afterward, the interaction locality is examined in terms of the plasma dispersion and the resultant spectral evolutions. And it is found that for pulse lengths larger than the plasma wavelength, the plasma-wave evolutions inside the pulse region result in the strong light phase-modulation along with the amplitude-modulation and whereby violation of the adiabatic description. The development of these phenomena is by production of the effective radiation back-reactions.

I. INTRODUCTION

The current ability in attaining short, ultra-intense laser pulses [1-2] has stimulated many extensive researches in the field of laser-matter interactions. Efforts are mainly conducted toward the construction of compact particle accelerators [3-10], bright X-ray sources [11, 12] and realization of conditions for the Fast Ignition (FI) scheme of Inertial Confinement Fusion (ICF) [13]. The propagation of intense laser pulse through the under-dense plasma is an important common part of all these scenarios. This subject has recently attracted a vast

number of attentions [8-10, 14-31]. The sub-critical densities are produced either due to the unavoidable pre-pulse effects in the laser solid interaction [3] or initially exist in the form of gas jets [26] or the state-of-the-art foam targets [27].

An important question related to the short intense laser pulse propagation through the sub-critical plasma is the nonlinear pulse evolutions. This issue is directly related to the interaction performance. In laser-plasma accelerators [8-10], it determines the dephasing length and the maximum attainable electron acceleration [21]. In laser interactions with high density plasmas, it is related to the plasma heating and particle acceleration [24-31].

In the case of very long pulse propagation through the plasma in the absence of wake excitation, the physics of light evolutions is well understood in the context of the relativistic generalizations of the common Raman and Brillouin scatterings [32-36]. However, in the presence of wake excitation by short laser pulses, the common scattering theories fail to describe the pulse evolutions (see e.g. Ref. [14]). This is because the simplifying concept of three (or four) wave interactions loses its applicability, as the strong wakefield couples an infinite number of the electromagnetic-spectrum components to each other. This complexity causes the subject of nonlinear pulse dynamics in the presence of the wake excitation to remain still as an open problem despite to the many existing theoretical works [14-23].

It is currently well-known that the laser pulse experiences nonlinear depletion due to the wake excitation [14, 15]. In addition, recent studies, related to ultra-short pulses (pulse lengths shorter than the plasma wavelength), have indicated that the problem shows new complexities in pulse evolutions [20] and new features like the wake amplification and the resultant plasma-wave phase velocity decrease behind the pulse [21]. But the obtained analytical results are limited to the early-time dynamics [21]. Moreover, the physics behind the complex system evolutions like the group velocity variations, pulse modulation and the plasma wake variations have remained poorly understood. Even more, a precise, reliable formula describing evolutions of the pulse group velocity due to the energy depletion is lacking in the literatures.

The important topic of the short pulse group-velocity, at relativistic amplitudes, has not yet received adequate attentions. To the best of our knowledge, the most important existing work on the topic is Ref. [37] which calculates *the rate of the total-energy transport* as the group velocity, without taking into account the pulse depletion. Apart from their being restricted to pulse lengths much longer than the plasma wavelength, the obtained results are of less interest in applications, as, the relation between the group velocity and the electron plasma-wave phase-velocity is lacking and complicated if would exist. Note, by calculating the group velocity, it is mostly desired to obtain the plasma-wave phase velocity (see e.g. Ref [20]).

The outlined unresolved problems in the full realization of the nonlinear pulse evolutions have been mainly originated from the previous inadequate modeling. A majority of previous works have used the Slow Envelope Analyses (SEA) to calculate the pulse variations [14-23] at very low plasma densities. The SEA presumes the wave solution in the form of $\psi(x,t)=\hat{\psi}(\xi,t)\exp(-i\omega_0 t+ik_0 x)$. Here $\xi\equiv x-v_g^0 t$, $v_g^0\equiv ck_0/\omega_0$ is the constant linear group velocity and ω_0 and k_0 are respectively the carrier frequency and wave-number obeying the linear dispersion relation $\omega_L^2(k)=c^2k^2+\omega_p^2$. The envelope function $\hat{\psi}(\xi,t)$ is supposed to vary very slowly with time, such that we have $\partial\hat{\psi}/\partial t << c\partial\hat{\psi}/\partial\xi \approx ck_p\hat{\psi}=\omega_p\hat{\psi}$. This assumption implies that the pulse carrier-frequency would remains very close to its initial value during the propagation, i.e. $\omega_0(t)\approx\omega_0(0)+\delta\omega(t)$ with $\delta\omega << \omega_p$. However in the case of intense pulse propagation through the plasma and in the presence of wake excitation, the radiation experiences strong redshift [14, 15, 21] and deceleration [21]. In our simulations it is observed that the redshift reaches the values comparable to the initial laser frequency at long times, causing the breakdown of $\delta\omega << \omega_p$. This phenomenon is a partial effect of the anomalous plasma dispersion in the fully nonlinear regime where very large evolutions of the spectral density along the dispersion curve may be observed. In this respect, the

SEA analyses presented previously [14-23] are either inadequate or, as mentioned in Ref. [21], describe only early stages of the pulse evolutions properly.

In this paper, we study the long-term nonlinear evolutions of an ultra-intense, short laser pulse due to the wake excitation inside the plasma by means of detailed Particle-In-Cell (PIC) simulations and new modeling and analyses. Our study is performed in one space -three velocity dimensions for p-polarized laser pulse. And pulse lengths both longer and shorter than the plasma wave length are considered. Our main purposes are to modify and further develop the present description of light evolutions. Especially we aim to shed light on the complex phenomena of pulse group velocity evolutions, pulse modulation [38, 39] and the transition from the stationary propagation into a semi-chaotic phase typically observed at high densities [24, 31].

It is turned out that the system shows adiabatic behavior as long as the plasma evolves very slowly in the Pulse Co-Moving (PCM) frame, due to the ignorable radiation back-reactions against the measured high plasma momentum. Note that this condition is radically different from assuming marginal variations for the laser carrier frequency, considered previously [14-23], as a very small variation in the group velocity can results in very high changes in this frequency. A sophisticated treatment of the adiabatic regime is presented, based on the proper application of the local conservation laws in the PCM frame in conjunction with the Lorentz

transformations. In this context, equations for the overall pulse evolutions are reduced into a single equation in terms of the global pulse group-velocity. This group velocity is found to be equal to the averaged plasma-wave phase-velocity in the pulse region, whence most relevant to applications compared to the previous results [37]. Due to the (here) proven equality between the local phase velocities of the plasma wave and the radiation, anomalies are observed in this regime, in the global group velocity and the plasma dispersion. The group velocity shows non-explicit density dependency and of remaining above the linear value over a long period of the propagation. These results are successfully examined against PIC simulations and their consistency with the other system evolutions and the physical intuition is fully discussed. Afterward, the interaction locality is examined in terms of the plasma dispersion and the resultant spectral evolutions. And it is found that for pulse lengths larger than the plasma wavelength, the plasma-wave evolutions inside the pulse region result in the strong light phase-modulation along with the amplitude-modulation and whereby violation of the adiabatic description. The development of these phenomena is by production of the effective radiation back-reactions.

This paper is organized in different sections. In Sec. II the governing equations are briefly outlined. In Sec. III, a basic overview of the problem is presented using PIC simulations, prerequisite to the proper modeling. In Sec. IV the adiabatic

regime of the interaction is described by solving the basic equations outlined in Sec. II and comparing with simulations. A complementary section (Sec. V) is devoted to discuss the non-adiabatic behaviors in the case of pulse lengths larger than the plasma wavelengths. Finally, the paper is concluded in Sec. VI.

II. GOVERNING EQUATIONS

The basic applied equations are the well known set of cold fluid equations plus Maxwell equations in the Coulomb gauge (in laboratory frame), $\nabla \cdot \mathbf{A} = 0$, as,

$$\frac{\partial n_q}{\partial t} + \frac{\partial n_q v_{qx}}{\partial x} = 0 \tag{1a}$$

$$\frac{\partial [\mathbf{p}_q + Q_q \mathbf{A}]}{\partial t} = -\nabla (m_e c^2 \gamma_e - e\phi) \tag{1b}$$

$$\frac{\partial^2 \phi}{\partial x^2} = -\frac{1}{\varepsilon_0} \sum_q n_q Q_q \tag{1c}$$

$$\frac{\partial^2 \mathbf{A}}{c^2 \partial t^2} - \frac{\partial^2 \mathbf{A}}{\partial x^2} = \frac{1}{\varepsilon_0 c^2} \sum_q n_q Q_q \mathbf{v}_q \tag{1d}$$

Here, n, $\mathbf{p}$, Q, ϕ and $\mathbf{A}$ stand for density, momentum, electric charge, scalar potential and vector potential, respectively. The subscript q indicates that the quantities are correspond to the component q^{th} (electron or ion) of the plasma. $\mathbf{v}_q = \mathbf{p}_q / m_q \gamma_q$ and $\gamma_q = (1 - \mathbf{v}_q . \mathbf{v}_q / c^2)^{-1/2}$ are the velocity and the relativistic

gamma factor, respectively. ε_0 and c are the vacuum permittivity and light speed, respectively.

It is shown in the supplementary materials that the set of equations (1) can result in the following covariant conservations laws [40],

$$\frac{\partial u_{EM}}{\partial t} + m_e c^2 \frac{\partial \gamma_e n_e}{\partial t} + c^2 \frac{\partial g_x}{\partial x} + m_e c^2 \frac{\partial \gamma_e n_e v_{ex}}{\partial x} = -e n_i \mathbf{v}_i \cdot \mathbf{E}, \qquad (2a)$$

$$\frac{\partial g_x}{\partial t} + m_e \frac{\partial \gamma_e n_e v_{ex}}{\partial t} + \varepsilon_0 \frac{\partial}{\partial x}[\frac{1}{2}E_y^2 + \frac{1}{2}c^2 B_z^2 - \frac{1}{2}E_x^2] + m_e \frac{\partial \gamma_e n_e v_{ex}^2}{\partial x} = -e n_i [E_x + v_{iy} B_z] \qquad (2b)$$

where subscripts e and i are respectively used for electrons and ions of a hydrogen type plasma. $u_{em} = \varepsilon_0 (E^2 + c^2 B^2)/2$ and $\mathbf{g} = \varepsilon_0 \mathbf{E} \times \mathbf{B}$ are the electromagnetic energy and momentum respectively ($\mathbf{E}$ and $\mathbf{B}$ are electric and magnetic fields respectively). We can neglect the contribution of $v_{iy} B_z$ compared to E_x in the right hand side of (2b), because due to their heavy mass, ions remain approximately immobile in the direction of the laser polarization.

The solution of equations (1a-1d) has been extensively considered in the previous studies of wake excitation by intense, short, laser pulses inside the tenuous plasma [41-44]. And a closed solution to these equations has been obtained within the so-called Quasi-Static Approximation (QSA) [41-45] which assumes that the plasma quantities are time-independent in the Pulse Commoving

(PCM) frame. Additionally, it is assumed that the pulse group velocity, v_g, remains constant. In this section we apply a new approach to QSA, useful for our future discussions and for clarifying the existing ambiguity on the concept of the PCM frame.

It has been frequently stated that the PCM frame is not a new real Lorentz-frame but it is the laboratory frame itself bearing some algebraic transformations (see e.g. Ref. [42]). This definition of the frame is both false and misleading. And it is crucial for our future discussions to clarify this ambiguity. In this way, we have explicitly shown in a separate supplemental material [46] that the common QSA equations could be obtained by assuming the time-independency in the *real* Lorentz boost PCM-frame and then transforming the reduced equations into the laboratory. The proof for this statement is straightforward but space-wasting. It can be easily realized by noting that the time-independency in the PCM frame means that quantities are only functions of $x|_{PCM}$. Since, according to the Lorentz transformations, $x|_{PCM} = \gamma_g (x - v_g t)$, time-space dependencies in the laboratory frame appear in the combination $x - v_g t$ (note γ_g is a constant in QSA), the main assumption made in the common QSA solutions. Here $\gamma_g = (1 - v_g^2 / c^2)^{-1/2}$ is the relativistic factor of the PCM frame and the notation $X|_{PCM}$ indicates that X is

measured in the PCM frame. Hereafter, this indication will be made for the PCM quantities and no special indication will be made for the laboratory quantities.

With the assumptions adopted by the QSA, the plasma optical effects which are entered through the current in the right hand side of (1d) are considered only through taking the constant group velocity, v_g, different from c. Therefore the wave equation (1d) is not explicitly solved and complexities in the plasma dispersion are avoided. The group velocity is usually taken equal to the linear value, v_g^0. In order to keep the paper consistency the necessary results of QSA solution of (1a-c) are summarized here.

Since, according to the QSA, quantities are time-independent in the PCM frame, solution of Eqs. (1a-1b) in this frame results in the conserved particle flux and energy,

$$n_e v_{ex}\big|_{PCM} = -v_g \gamma_g n_{e0}, \tag{3a}$$

$$[\gamma_e m_e c^2 - e\phi]\big|_{PCM} = \gamma_g m_e c^2. \tag{3b}$$

In the right hand sides of Eqs. (3a-3b) we have used the fact that the undisturbed-plasma flows toward the pulse region with velocity $-v_g$ in the PCM frame. In (3a), we have also used the relation $n_{e0}\big|_{PCM} = \gamma_g n_{e0}$ for the undisturbed electron density

in the PCM frame, with n_{e0} being the undisturbed electron density in the laboratory frame.

It can be easily shown using the Lorentz transformations that the equations (3a-3b) are equivalent to the well-known equations $n_e(\beta_g - \beta_{ex}) = n_{e0}\beta_g$ and $\gamma_e m_e c^2(1-\beta_g\beta_{ex}) - e\phi = 1$ given in literatures (see e. g. Ref. [42]). Here $\beta_g \equiv v_g / c$ and $\boldsymbol{\beta}_e \equiv \mathbf{v}_e / c$. Using these equations together with $\gamma_e\beta_{ey} = a_y$ ($\mathbf{a} \equiv e\mathbf{A}/m_e c$) obtained from the conservation of the transverse canonical momentum, the right hand side of the Poisson equation (1c) is expressed in terms of ϕ. The resultant equation is then integrated to give the electric field and the electric potential in the disturbed region. Moreover, behind the pulse, $a_y = 0$ and Eq. (1c) gives a first integral,

$$E_x^2 + 2(\gamma_e - 1)E_p^2 = E_w^2 \tag{4}$$

where $E_p = m_e c\omega_p / e$ and E_w is the wakefield amplitude.

III. A BASIC PIC-SIMULATION OVERVIEW OF THE INTERACTION

In this section, and before going to comprehensive analyses, a basic overview of the problem is presented using PIC simulations. Different interaction regimes at different physical parameters are characterized and new uncovered or un-

emphasized aspects of the problem which are necessary to proper modeling and its understanding are outlined.

Our simulations are carried out using a 1D3V PIC code written by J. Yazdanpanah [43, 44]. In addition to the common capabilities of PIC codes, this code is equipped with utilities for detailed spectral and plasma dispersion analyses. Moreover, a utility has been added to calculate the QSA solution of Eqs. (1a-1c) at any desired time using the *instantaneous* vector-potential profile extracted from the direct PIC simulations [44]. The numerical integration of (1a-1c) has been done using the fourth-order Runge-Kutta method. The obtained solution is, in fact, the system *adiabatic solution* for the plasma wave and is significant in this study. The adiabaticity is due to the fact that the devised approach is equivalent to treat the time argument of a_y as a parameter in the PCM frame, i.e. the pulse is assumed time-independent during a small time period which is still sufficient for the plasma to pass several plasma wavelengths.

We have performed many long-term simulations in order to understand the system behavior at different applied physical parameters. Four instances of these simulations will be presented in this study. In all simulations, the laser wavelength and the peak value of the dimensionless amplitude are respectively fixed to $\lambda = 1\mu m$, $a_0 = 2$. The initial plasma profile is step-like and the initial electron and

ion temperatures are set to $k_B T_e / m_e c^2 = 10^{-4} (\sim 50\text{eV})$ and $k_B T_i = 0$ (k_B is Boltzmann constant), respectively. The size of simulation box is 600 λ, with open

Table I : summary of PIC simulations.

Simulation	**Plasma density** n_{e0} / n_c	**Pulse duration** τ_L[fs]	**Pulse profile (TL3,TL2 ,TL1) [fs]**
S1	0.01	60	(30,0,30)
S2	0.01	100	(30,40,30)
S3	0.03	60	(30,0,30)
S4	0.03	60	(18,24,18)

and reflective boundary conditions being applied at its ends for the fields and particles, receptively. The mesh cell is λ/200 and initially contains 64 macro-particles per cells. Plasma is initialized in the position range $[40\lambda, 580\lambda]$ and the total simulation run time is set as $t = 1.8\text{ps}$. Other parameters of these simulations are summarized in table I. These parameters have been chosen in such a way that the significances of the plasma density, the pulse duration and the scale lengths of the pulse envelope could be realized. The meanings of the table headings used in the first to third columns are clear. The fourth column describes the pulse profile. In general, the pulse envelope consists of a flat-top central part with *TL2* duration sided by two sinusoidal-shape rising and falling parts, each with *TL1* and *TL3* duration. By sinusoidal form we mean, for example, that the rising part of envelope

at $t = 0$ is described by $\sin(\pi(x - x_r) / c.TL1)$, with x_r being a proper position bias. *TL2=0* means that no flat-top is included and the envelope has the pure sinusoidal form.

The pulse length in *S1* has been shorter than the plasma wavelength, $L_p \approx \lambda_{\mathrm{p}}^{\mathrm{NL}} / 2$ (L_p is the pulse length and $\lambda_{\mathrm{p}}^{\mathrm{NL}}$ is the relativistic, nonlinear plasma wavelength [42]), while in other simulations the situation is the reverse, i.e. $L_p > \lambda_{\mathrm{p}}^{\mathrm{NL}}$. It is well-known that when the condition $L_p > \lambda_{\mathrm{p}}^{\mathrm{NL}}$ is satisfied the so-called pulse modulation [38, 39] will be observed, though the physics behind the phenomenon is not well understood. When the envelope scale lengths, $c \cdot TL1$ and $c \cdot TL2$ are both smaller than $\lambda_{\mathrm{p}}^{\mathrm{NL}}$, a region of a periodic wakefield will be produced inside the flat-top part of pulse envelope. This is the case in *S4* and *S2*.

A brief overview of the spatiotemporal laser pulse evolutions at the lower plasma density, used in *S1* and *S2*, is presented in Fig. 1. Here, the mid-term profile of the vector-potential, a_y, is plotted for each simulation together with three snapshots of the Poynting-vector, $\mathbf{g}$, at three different times. Also, at each panel, the initial profile of each plotted issue is given for the comparison purpose. Furthermore, in $\mathbf{g}$-panels, we have plotted the corresponding profile of the plasma wave energy, $C_w \equiv (E_x / E_p)^2 + 2(\gamma_e - 1)$ (with reversed sign and shifted by 1, for

clarity). Panel (e) contains additionally the instantaneous plot of the electron density as a representative of the plasma wave. C_w shows the magnitude of the excited wake; it varies inside the pulse and reaches the constant value of $(E_w / E_p)^2$

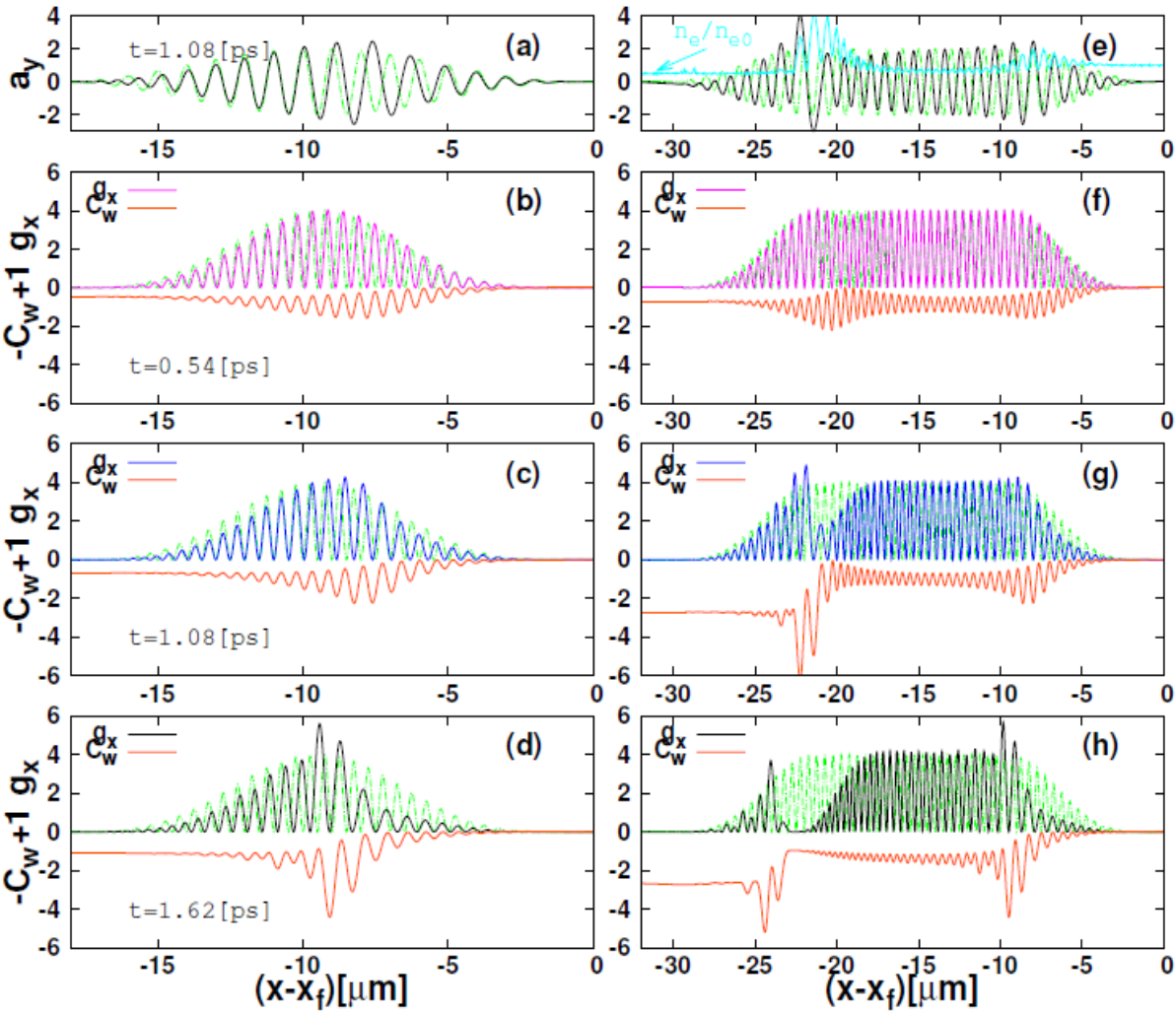

FIG. 1. (Color online): The vector potential profile at t=1.08ps (black) at initial time (green) panel (a), the Poynting vector (pink), wake-excitation profile with reversed sign (orange) at three different time instances t=0.54ps, panel (b), t=1.08ps, panel (c) and t=1.62ps, panel (d) -in addition the initial Poynting vector (green) is shown in panels (b-d)- for simulation *S1*. In panels (e-h) the same issues are represented for simulation *S2*. In panel (e) the profile of electron density (blue) is also presented.

behind the pulse (see Eq. (4)). Also, its spatial gradient shows the magnitude of the local wake excitation. Comparison between this gradient and **g** in panels (b-d) & (f-h) shows that the laser pulse generally experiences the down-chirp in the locations of positive wake excitation (positive gradient of C_w-envelope) and vise versa in the locations of the negative wake excitation (negative gradients of C_w-envelope). Also it is observed that the radiation flows in the opposite direction of gradient of C_w-envelope, being accumulated at descents of this envelope and eroded in their neighborhoods. In this respect the C_w-envelope acts as an effective potential for the radiation. The dynamics of *S3* and *S4* (not shown in Fig. 1) in the initial stages of interactions is the same as *S2*.

An important, unexpected phenomenon which occurs when $L_p > \lambda_{\mathrm{p}}^{\mathrm{NL}}$ and is observed in C_w plots of Figs. (1f-1h), in the case of *S2*, is the development of local wake excitation in the locations of the electron density peaks and inside the initially uniform part of the pulse envelope. (to find the peak locations, compare the density profile in Fig. (1e) to the instantaneous intensity profile in Fig. (1g)). Note that QSA predicts no excitation inside the flat parts of the envelope. This phenomenon has become possible because an unexpected modulation occurs at the density-peak location that deforms the initially constant part of the pulse. We used the term “unexpected” because, initially, there does not exist any C_w-gradient in

the peak location in order to derive the radiation evolutions. The radiation plots (a_y, $\mathbf{g}$) in Figs. (1e-1h) shows that the modulation is such that the radiation is accumulated behind the density peak and spread in its front. In the absence of initial deriving force, this phenomenon could become possible only by the forward flow of the radiation with respect to the plasma wave, or, equivalently, backward flow of the plasma through the radiation, and via the phase modulation [16].

The temporal evolution of the radiation (a_y) spectral density is given in Fig. 2 for simulations summarized in Tab. I. In the case of *S1* (panel (a)), it is obviously observed that the central wave-number, k_0, is continuously decreased along with the spectral-broadening increase. In the case of *S2* (panel (b)), the decrease in the central mode is much weaker with respect to *S1*, as, initially, the wake excitation is performed by a much smaller part of the pulse compared to *S1*. Instead, the so-called electromagnetic-cascading [38, 47, 48] is observed in a strong form, i.e. certain, equally-spaced modes grow out of the whole spectrum. In the case of *S4* (panel (d)), the cascading occurs at early times in the same way as *S2* and in the spite of *S3* (panel (c)). This is due to formation of periodic wake profiles inside the flat-top parts of respective pulses in *S2* and *S4* and vise versa for *S3*. For all cases with $L_p > \lambda_{\mathrm{p}}^{\mathrm{NL}}$, including *S2*, *S3* and *S4* (panels (b-d)), the spectrum takes a very broad shape almost decreasing with the wave-number (maximum at zero) at

sufficiently large times. However, the time needed to reach this stage decreases with the density increase.

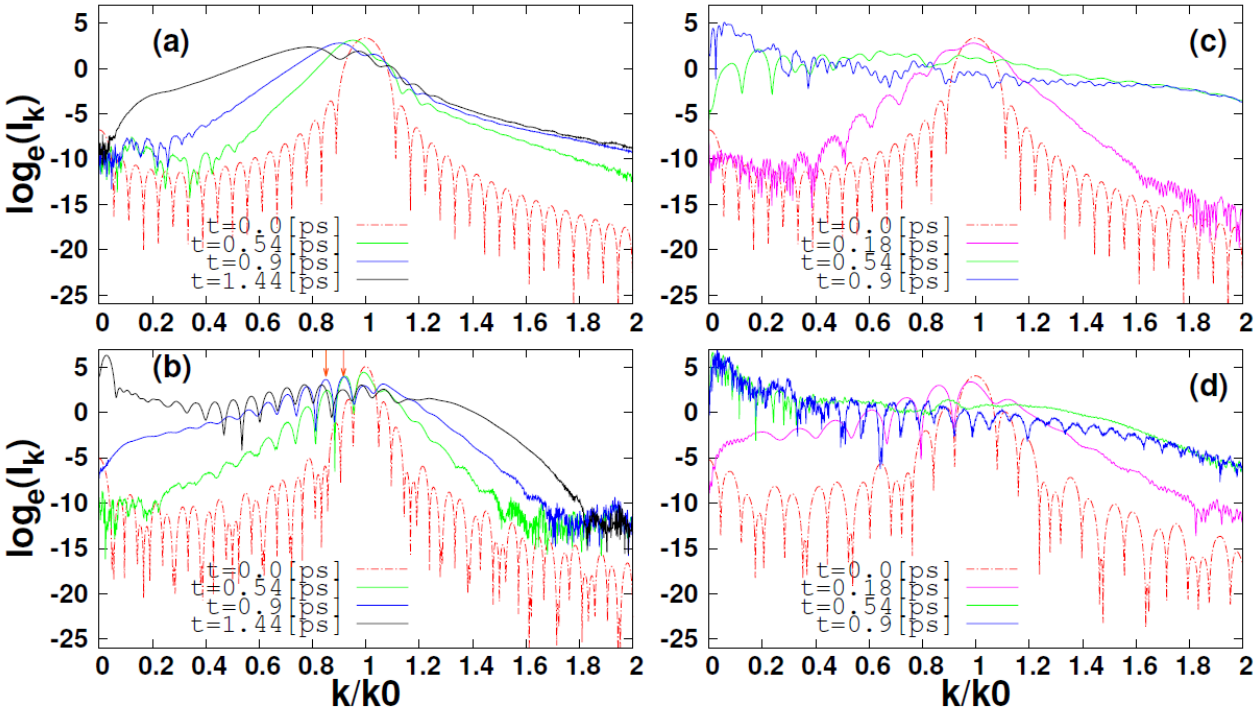

FIG. 2. (Color online): Spectral density of the vector potential (a_y), vs normalized wave number for four simulation cases at four moments. Simulation cases S1 panel (a) and S2 panel (b) are studied at time t=0.0 (red-dashed line), t=0.54ps (green-solid line), t=0.9ps (blue-solid line) and t=1.44ps (black-solid line), and simulation cases S3 panel (c) and S4 panel (d) are studied at time t=0.0 (red-dashed line), t=0.18ps (pink), t=0.54ps (green-solid line) and t=.9ps (blue-solid line).

In Fig. 3 we have compared the *adiabatic solution* of Eqs. (1a-1c), for the plasma wave, with the direct PIC simulation results at two different times, for simulations *S1* (panels (a-c)) and *S2* (panels (d-f)). Panels (a-b) and (d-e) represent the electric-field profiles for *S1* and *S2*, respectively, and panels (c) and (f) show the corresponding longitudinal phase-space, plotted at the longer time moment.

Note that, the a_y profile used in the adiabatic solution contains all evolutions up to the plot time. In this figure, it is observed that for *S1*, the adiabatic solution is in

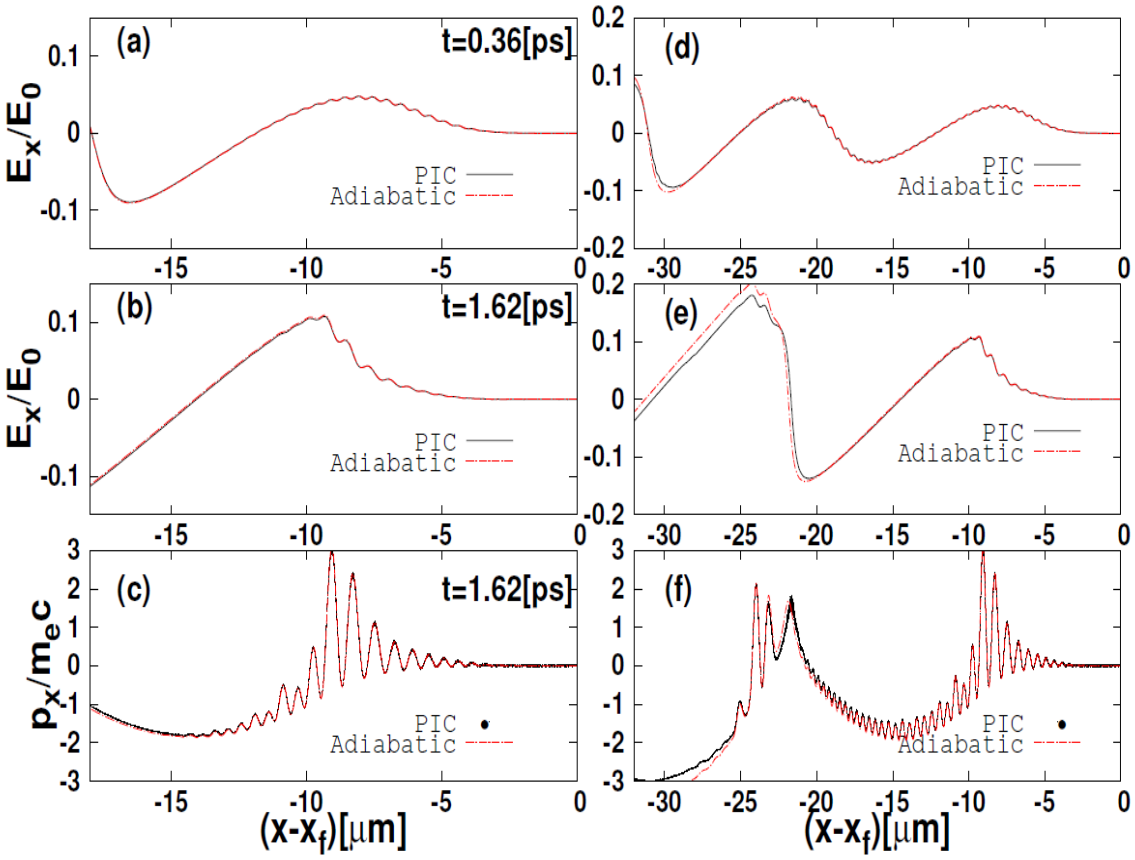

FIG. 3. (Color online): Adiabatic solution (red-dashed line) and direct PIC simulation results (black-solid line) of normalized wakefield profile at moment t=0.36ps for simulation *S1* panel (a) and *S2* panel (d). And at moment t=1.62 for simulation cases *S1* panel (b) and *S2* panel (e). Panels (c) and (f) show the adiabatic (red-dashed line) and PIC simulation (black-solid points) results for the longitudinal phase-space at t=1.62 for *S1* and *S2* respectively.

the precise agreement with the direct simulation results in the pulse region. The situation is the same for the most parts of pulse region in the case of *S2*, but an small deviation is observed to starts from the location of the pulse modulation at relatively long times ($t = 1.62\text{ps}$). The coincidence of locations of the deviation

onset and the pulse modulation can be confirmed by comparing Figs. (3f) and (1h). This shows that the violation of the adiabatic description in the pulse region is related to the pulse modulation. Other deviations observed behind the pulse in Fig. (3f) are related to the electron trapping.

An important feature observed on Fig. 3 and more clearly in the phase plots (c) and (f), is the local equality between the phase-velocities of the laser pulse and the electron plasma-wave. Otherwise, we should observe, for example, mismatching in corresponding locations or dissimilarities between the shapes of density peaks in different solutions, as the laser would oscillate in the local plasma-wave phase frame. This observation contradicts with the frequently stated equality of the plasma-wave phase-velocity and the *electromagnetic* pulse group-velocity in the previous studies of laser interaction with sub-critical plasma (see e.g. [4-7], [14-20]). The contradiction arises as the phase velocity of electromagnetic modes is always larger than their group velocity. As it is now clear, observed equality between the phase velocities is the basis for the new approach introduced in the previous section for derivation of QSA equation. The observed phenomenon will be expanded in details in Sec. IV. To avoid confusion, the reader should notice that the laser pulse is a pure radiation and not a packet of electromagnetic modes, therefore its local phase and group velocities may equal.

In Fig. 4, the effects of the plasma-density increase are summarized by plotting the simulation results in the case of *S3*, performed at a higher plasma density, $n_{e0}/n_c = 0.03$, and almost with the same ratio of the pulse-length to the plasma wavelength as *S2*.

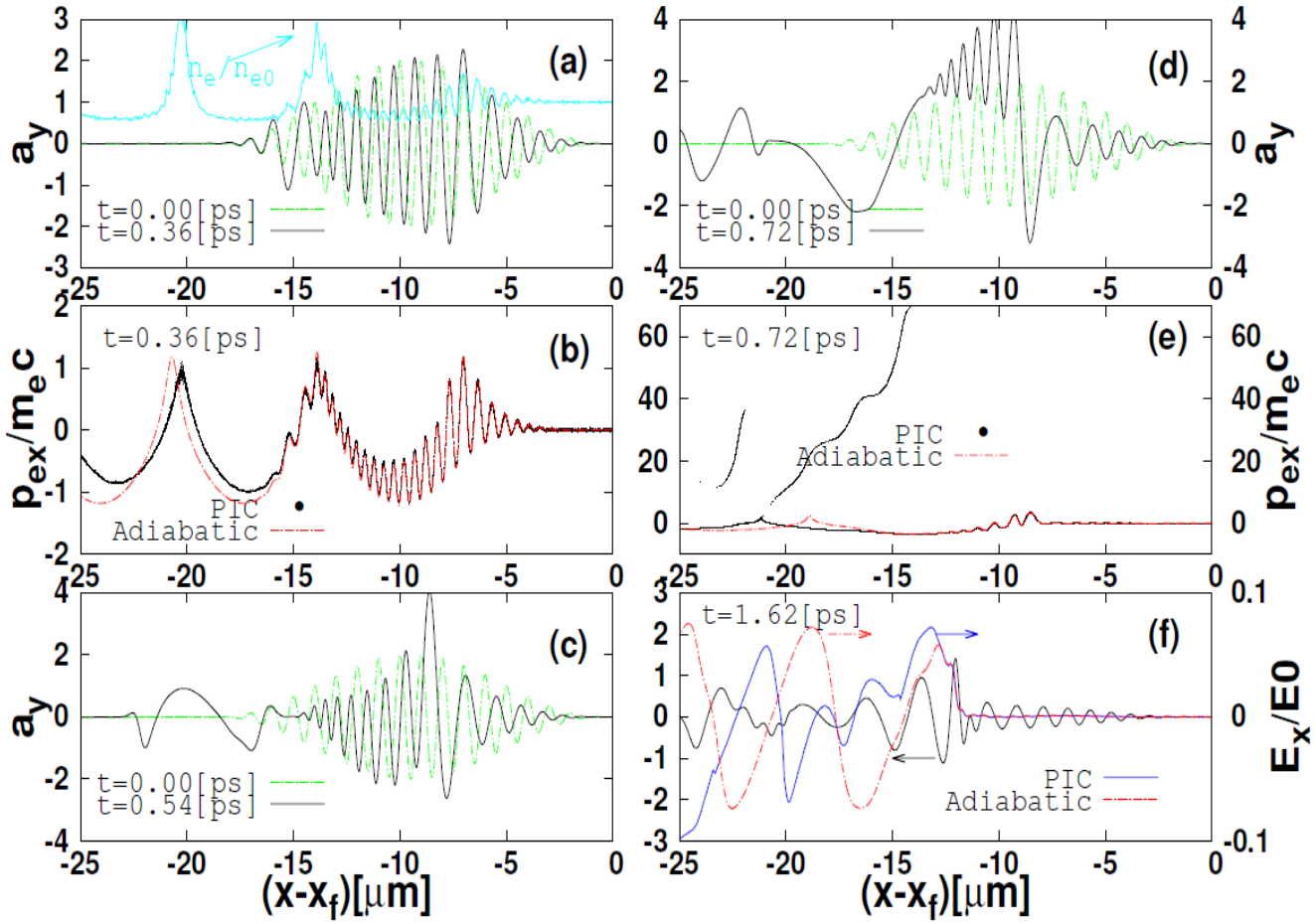

FIG. 4. (Color online): The profile of the vector potential a_y (black-solid line) at given moments together with the initial profile (green- dashed line), panels (a, c, d). The simulation results (black-dotted line) and the adiabatic solution (red-dashed line) for the longitudinal phase-space at different times, panels (b, e). The long-time profile of a_y (black-solid line) together with the corresponding simulation results (blue-solid line) and the adiabatic solution (red-dashed line) for the wakefield profile, panel (f)- all for the simulation case *S3*.

It is observed that the early stages of pulse evolutions (panel (a) at $t = 0.36\text{ps}$) are the same as the longer-time evolutions in the case of *S2*, with the same mechanism for the modulation (compare Figs. (3a) versus (1e)). Also, the comparison between the adiabatic and PIC results, given in panel (b) at $t = 0.54\text{ps}$, shows the same characters as Fig. (3f) given for *S2* at the longer time $t = 1.62\text{ps}$. The difference observed here between *S2* and *S3,* is that the modulation develops faster in *S3* with respect to *S2*. To be convinced, notice that for *S2* and according to Fig.(1f), the modulation starts approximately at $t = 0.54\text{ps}$. This is while $t = 0.36\text{ps}$ is nearly the final stages of the modulation for *S3*, as, when the time further proceeds (panel (c) at $t = 0.54\text{ps}$), we observe the formation of a tail of large-wavelength in the radiation, a phenomenon which is also observed at the final stages of *S2* (not shown here). When, again, the time is sufficiently increased in *S3* (panels (d-e) at $t = 0.72\text{ps}$), the kinetic effects come to play in terms of electron-trapping, highly affecting the radiation and the plasma wave and causing noticeable deviation from the adiabatic theory. Eventually (panel (f) at $t = 1.62\text{ps}$), the pulse is largely deformed, the agreement between the two solutions is lost behind a small region near the pulse front and the phase relation between the plasma and electromagnetic waves is completely destroyed. The same behavior is expected for lower densities at longer times.

In addition to above observation, we could also observe the recently observed (see e.g. ref [21]) phenomena like large wakefield-amplification and resultant plasma wave phase deceleration behind the pulse (Fig 3).

IV. ADIABATIC THEORY OF PULSE EVOLUTIONS

A. THE MODEL DESCRIPTION

Suppose that the plasma evolves very slowly in the PCM frame. This is the case when the radiation back-reactions exerted on the plasma as the response to the radiation evolutions are ignorable in the PCM frame. Quantitative estimations of necessary conditions for this situation need prior calculations of the radiation evolutions. Therefore, these estimations are postponed to after the mentioned calculations. Nevertheless, the established assumption can be understood intuitively by noting the fact that the radiation momentum is highly decreased in the PCM frame due to the strong Doppler down-shift while the plasma momentum is highly up-boosted. Therefore, even a total back-reflection of the radiation by the plasma stream may not introduce a noticeable change in the plasma momentum. Our simulations results, presented in the previous section, confirm the validity of this assumption during the long term propagation of ultra-short pulses and, at least, at early time stages of propagation of pulses with lengths larger than the plasma wavelength (see Fig.3 and corresponding descriptions). The proposed assumption

does not necessitate ignoring the carrier-frequency (wave-number) variations due to pulse deceleration, despite to SEA.

Under the established assumption, the set of equations (3a-3b) remains approximately valid about the plasma. In addition, we can set in equations (2a) and (2b), $\partial\gamma_e n_e / \partial t\big|_{PCM} \approx 0$, $\partial\gamma_e n_e v_{ex} / \partial t\big|_{PCM} \approx 0$, $\partial\phi / \partial t\big|_{PCM} \approx 0$ and $\partial A_x / \partial t\big|_{PCM} \approx 0$ (note that $A_x\big|_{PCM} = -\gamma_g \beta_g \phi / c = -\beta_g \phi\big|_{PCM} / c$ due to the gauge condition $A_x = 0$ in the laboratory frame) . By applying these simplifications we obtain,

$$\{\frac{\partial u_{EMT}}{\partial t} + \frac{\partial}{\partial x}[c^2 g_x - n_{e0} m_e c^2 \gamma_g v_g \gamma_e + n_{e0} e \gamma_g v_g \phi] = 0\}\Big|_{PCM}, \tag{5a}$$

$$\{\frac{\partial g_x}{\partial t} + \frac{\partial}{\partial x}[\frac{\varepsilon_0}{2} E_y^2 + \frac{\varepsilon_0}{2} c^2 B_z^2 - \frac{\varepsilon_0}{2} E_x^2 - n_{e0} m_e v_g \gamma_g \gamma_e v_{ex} - e n_{e0} \gamma_g \phi] = 0\}\Big|_{PCM} \tag{5b}$$

where we have made use of Eq. (3a), $\mathbf{E} = -\nabla\phi - \partial\mathbf{A} / \partial t$ and the facts that $v_{ix}\big|_{PCM} \approx -v_g$ and $n_i\big|_{PCM} \approx \gamma_g n_{e0}$ due to the heavy ion mass. u_{EMT} is defined to be $u_{EMT} = \varepsilon_0 (E_\perp^2 + c^2 B_\perp^2) / 2$. The second term in the right hand side of Eq. (2b) has been neglected in arriving to Eq. (5b) according to arguments given below Eq. (2b).

Eq. (5a) can be further simplified by using equation (3b) and gives,

$$\{\frac{\partial u_{EMT}}{\partial t} + c^2 \frac{\partial g_x}{\partial x} = 0\}\Big|_{PCM} . \tag{6a}$$

This equation describes the energy conservative light flow through a *preformed* density profile. This is consistent with the fact that the plasma mechanical-energy and more generally the plasma profile does not vary with time in the PCM frame.

By eliminating ϕ in Eq. (5b) using Eq. (3b), and applying the Lorentz transformations $E_x = E_x\big|_{PCM}$ and $\gamma_e = \gamma_e\gamma_g(1+v_g v_{ex}/c^2)\big|_{PCM}$ in the obtained result, equation (5b) reads as,

$$\{\frac{\partial g_x}{\partial t} + \frac{\partial u_{EMT}}{\partial x} = \varepsilon_0 E_p^2 \frac{\partial C_W}{\partial x}\}\Big|_{PCM} \tag{6b}$$

Eq. (6b) states that the local light-momentum varies with time due to the convection ($-\partial u_{EMT}/\partial x$ term) and the wake excitation ($E_p^2 \partial C_W/\partial x$ term). The overall effect of the convection term is zero. Therefore, it does not affect the overall depletion and the spectrum evolutions. Eq. (6b) is, in fact, the mathematical description of arguments given on Fig. 1.

The overall variations of the wave momentum and energy are obtained by integration of Eqs. (6a) and (6b) over x. In this way, we obtain in the PCM frame,

$$\frac{dH_{FT}}{dt}\Big|_{PCM} = 0, \tag{7a}$$

$$\frac{dK_F}{dt}\Big|_{PCM} = -\frac{1}{2}\varepsilon_0 E_w^2 \tag{7b}$$

where $H_{FT} = \int_{-\infty}^{\infty} \mathrm{dx} u_{EMT}$ and $\mathbf{K}_F = \int_{-\infty}^{\infty} \mathrm{dx}\mathbf{g}$ are the total electromagnetic energy and momentum respectively. Based on the principles of relativity theory, the energy (H_{FT}) and the momentum $(\mathbf{K}_F)$ of a localized electromagnetic disturbance form a four-vector [49], say $\mathbf{K}_4$, which always can be written in the covariant form of $\mathbf{K}_4 \equiv (H_{FT}, c\mathbf{K}_F) = H_0(\gamma_g, \gamma_g \mathbf{v}_g)$. Here $\mathbf{v}_g$ is the global electromagnetic group velocity,

$$\mathbf{v}_g = \frac{c^2 \mathbf{K}_F}{H_{FT}}, \tag{8}$$

and $H_0 \equiv H_F\big|_{PCM}$ is the electromagnetic energy in PCM frame. $\mathbf{v}_g$ has been implicitly used earlier in this paper in defining the PCM frame prior. Its relation (8) gives *the rate of radiation energy transport*, despite the corresponding definition in [37]. H_0 takes the role of the particle rest mass when the electromagnetic disturbance as whole is treated as a particle. With assumptions made in this section, we have obtained $dH_0 / d\tau = 0$ (Eq. (7a)) with $\tau \equiv (t)\big|_{PCM}$ being the proper time. Therefore, analogous to the relativistic particle dynamic [49], we can readily apply (7b) in the laboratory frame, i.e.

$$\frac{dK_F}{dt} = -\frac{1}{2}\varepsilon_0 E_w^2. \tag{9a}$$

We should notify that Eq. (9a) has been obtained and used previously in Refs [20, 21] via SEA. The reason for this accidental coincidence, despite to the outlined essential difference between our approach and SEA (see the introduction), is that the force term (right hand side of (9a)) has not explicit dependencies on the pulse parameters. Nevertheless, our approach still gains over the SEA, at least, by two reasons. Firstly, the physics is modeled correctly here, with less restricting and more examinable assumptions; this allows for more adequate characterization and understanding of the non-adiabatic regime. Secondly, and more importantly, we can go further and calculate the global group velocity, as we have the relation between the radiation energy and momentum.

Using $c\mathbf{K}_F = H_0\gamma_g\mathbf{v}_g$ from $\mathbf{K}_4$ presentation, the identity $d[\gamma_g\beta_g]/dt = \gamma_g^3 d\beta_g/dt$ ($\beta_g = v_g/c$) and noting the constancy of H_0, Eq. (9a) takes the form of,

$$\frac{d\beta_g}{dt} = -\frac{1}{2}\frac{\varepsilon_0 c\gamma_{g0}E_w^2}{\gamma_g^3 U_{P0}}. \qquad (9b)$$

Here, $U_{p0} = \gamma_{g0}H_0$ is the initial pulse energy and γ_{g0} is the initial group-velocity gamma-factor. Equation (9b), derived for the first time in this work, fully describe the pulse evolutions in the adiabatic regime. It states that the pulse is slowly decelerated and loses its energy. Due to the deceleration, the pulse energy

in the PCM frame decreases with time despite to energy conservation in the PCM frame. When the evolutions of the wake amplitude, E_w, are ignored, for example at early times, the solution of Eq. (9b) is obtained in the form,

$$\beta_g = \sin[\tan^{-1}(-\frac{t}{\tau_0} + \alpha)], \tag{9c}$$

where $\tau_0 \equiv 2U_{P0} / \varepsilon_0 c\gamma_{g0} E_w^2$ and $\alpha \equiv \tan[\sin^{-1}[\beta_{g0}]]$. With this solution the depletion time is given by $\tau_d = \alpha\tau_0$ (when $\beta_g = 0$) which differs from previous estimates [14, 21] in the way that it takes into account the near c being of the initial group velocity. Moreover, it is noticed that despite to the linear group velocity, the obtained result (9c) does not show the explicit density dependency. Also, because $\beta_{g0} \approx 1$ (the pulse is initiated in the vacuum) and $\gamma_{g0} >> 1$, α and $\omega_p \tau_d$ tend to very large values. Therefore, due to very smooth variations of $\tan^{-1}$ at its large arguments it is expected that β_g reaches the linear value, $v_g^0 / c \equiv ck_0 / \omega_{0L} = \sqrt{1 - n_{e0} / n_c}$ after a very long time. This phenomenon will be further discussed in the next two subsections.

B. DEPLETION AND VARIATIONS IN CARRIER WAVE-NUMBER, WAKE-AMPLITUDE AND GROUP VELOCITY

An important feature of the pulse evolutions is the temporal variations of the carrier frequency and wave-number, $\omega_0(t)$ and $k_0(t)$. The equality of the local phase-velocities of the plasma-wave and the laser-pulse, pointed out in Sec. III on Fig. 3, implies the light frequency to be approximately zero in each local phase frame of the radiation. If, in addition, it can be assumed that every local frame in the radiation region moves approximately with the same velocity as the global PCM frame (no serious phase-modulation, a subject which will be discussed in Sec. V),we will have $[\omega_0 \approx 0]\big|_{PCM}$. With this equation, simple expressions can obtained for $\omega_0(t)$ and $k_0(t)$ via Lorentz transformations, i.e. $\omega_0 \approx \gamma_g \beta_g c(k_0\big|_{PCM})$ and $k_0 \approx \gamma_g (k_0\big|_{PCM})$. Further, if we confine ourselves to early times for which the $k_0\big|_{PCM}$ has not yet changed noticeably, we readily obtain,

$$\omega_0(t) = \frac{\gamma_g \beta_g}{\gamma_{g0}\beta_{g0}}\omega_0(t=0),\ \mathbf{k}_0(t) = \frac{\gamma_g}{\gamma_{g0}}\mathbf{k}_0(t=0). \qquad (10)$$

The above equation is also derived for the first time in this paper and via the substitution of β_g from (9b) or (9c) gives the early time evolutions of the carrier frequency and wave number. It states that the overall pulse depletion is accompanied by the carrier-frequency (wave-number) down-shift. Furthermore, by putting the obtained equations together with the relation $(H_{FT}, c\mathbf{K}_F) = H_0(\gamma_g, \gamma_g \mathbf{v}_g)$ and assuming $\beta_g \approx 1$ for early times, we obtain the

familiar adiabatic relations $H_{FT}(t)/\omega_0(t) = \text{constant}$ and $K_F(t)/k_0(t) = \text{constant}$. These equations have similarities with the adiabatic equation obtained in Ref. [15] via the SEA. This coincidence is natural by the facts that the validity of these equations is restricted to early times or to very weak wake excitations. And they are obtained under the ignorance of group velocity variations (setting $\beta_g = 1$ in Eq.(10) for $\omega_0(t)$), implicitly assumed by the SEA.

According to the early time equation, $H_{FT}(t)/\omega_0(t) = \text{constant}$, and the electromagnetic energy relation in terms of a_0 and ω_0, $H_{FT}(t) = \eta(t)a_0^2(t)\omega_0^2(t)$, we obtain $\eta a_0^2\omega_0 = \text{constant}$ where η is the pulse shape factor. As long as the pulse shape has not changed seriously ($\eta(t) \approx \eta(0)$), we obtain $a_0^2(t) = a_0^2(0)\omega_0(0)/\omega_0(t)$ which predicts the amplification of the pulse peak amplitude along with the frequency redshift. This in turn causes the amplification of wake amplitude as discussed in Ref [20, 21]. Both the pulse-peak and the wakefield amplifications are observed in our simulation results in Figs. (1 and 3) and in the history plots of Fig. (5). However, the pulse shape evolutions could be quite large at long times as observed in plots in the previous section (see Figs. 1 & 2 and related descriptions). And obtaining an expression for pulse shape which remains valid at long times needs full solution of the wave equation in the PCM frame which seems impossible.

In this work, the wakefield evolutions have been extracted from the simulations and via the adiabatic solution of equations (1a-1c) as described in Sec. III. In Fig. 5, the time histories for the electromagnetic energy-momentum and the wakefield amplitude are presented form simulations *S1* (a) and *S2* (b) and *S3*(c). Also, are presented the analytical results from integration of Eq. (9a), performed using the simulation results for the time history of E_w (the adiabatic solution of the plasma wave). In the case of *S1*, the wake amplitude grows monotonically during the simulation time and the excellent agreement is observed between the simulation and the analysis for the energy-momentum. In *S2* and *S3* the agreement is also perfect in the range of regular E_w variations. After a long time-period in the case of *S2*, and a shorter period in the case of *S3*, the $E_w$history takes an irregular oscillatory pattern and, in the same time, the agreement between the simulations and the adiabatic results for the energy-momentum is lost. This shows the violation of the adiabatic conditions at the deviation onset. Since the norm of the radiation four-momentum, $H_0^2 = H_{FT}^2 - c^2 K_F^2$, is approximately zero ($H_0^2 = U_{p0}^2 / \gamma_{g0}^2 << H_{FT}^2$), as long as the pulse energy is not largely depleted, H_{FT} / c approximately equals K_F as is observed in Fig. 5. The unexpected deviation which is observed at long times in the case of *S3* is, again, related to the

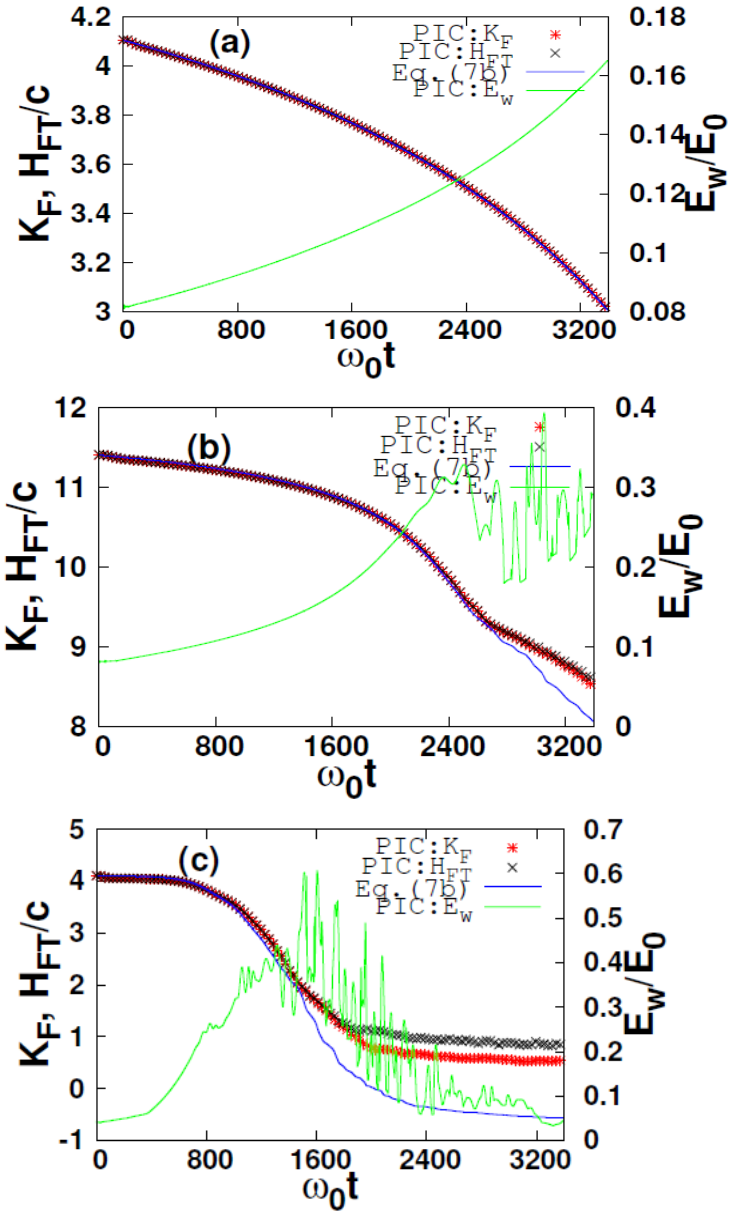

FIG. 5.: time histories of the electromagnetic energy, H_{FT}, (black-cross line), electromagnetic momentum, K_F, (red-star line) and wakefield amplitude E_w (green-solid line) of simulation cases *S1* panel (a), *S2* panel (b) and *S3* panel (c). And time histories of electromagnetic momentum K_F form adiabatic solution of Eq. (9a) for simulation parameters of all cases (blue-solid line)

violation of the adiabatic conditions. The simulation *S4* does not show distinctive features superior to *S3*, hence it is not discussed here.

In Fig. (6a), we have plotted the β_g history both from formula (9c) (constant E_w) and from direct integration of (9b) (variable E_w), for *S1*. It is observed that including the E_w-variations is very important. The linear value for the group velocity, including the relativistic mass corrections, is given by $\sqrt{1-n_{e0}/<\gamma_L>n_{cr}}$ ($<\gamma_L>\equiv\sqrt{1+a_0^2/2}$) and assumes the value 0.997 in the case of *S1*. It is seen that β_g anomalously remains very close to the unity and above this linear value over a considerably long time period.

The precise direct-detection of the small variations in β_g , observed in Fig. (6a), via PIC simulations is impossible due to the finite grid spacing, i.e. accurate measurement of the changes needs ultra-fine resolution of the space which, in turns, makes the long-term simulations cumbersome. Therefore, direct comparison with simulation results has not been made for this quantity. Nevertheless, the conformation of the analyses in the case of energy-momentum, described on Fig (5), guaranties the validity of the formula (9b). Additionally, the comparison between the formula (10), for the carrier wave-number, and corresponding simulation results can be utilized to further approve Eq. (9b) for β_g. Since, the

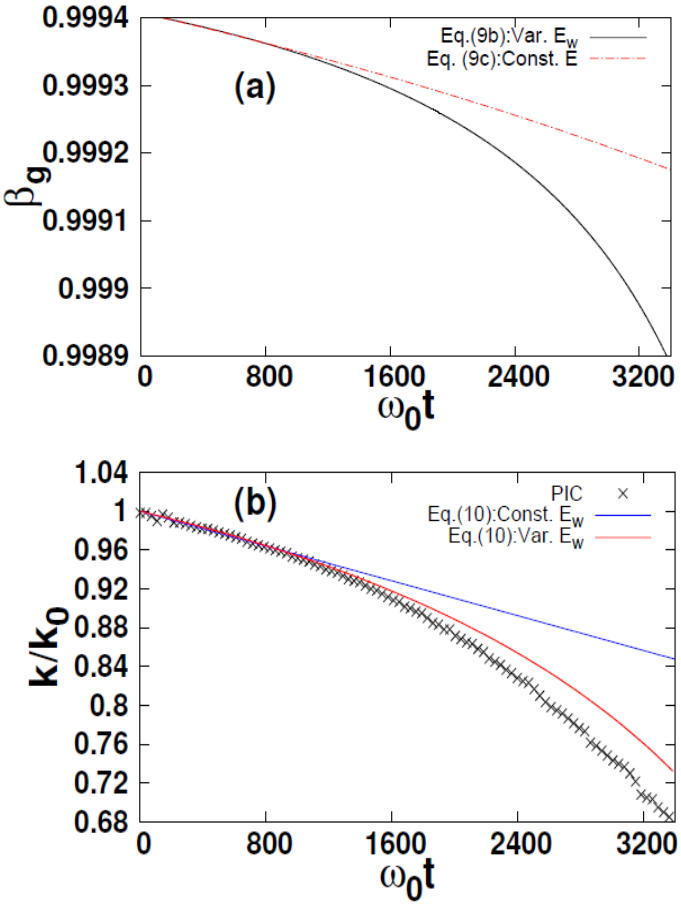

FIG. 6. (Color online): Time history of the group velocity in the case of parameters of *S1* from formula (9c) with constant E_w (red-dashed line) and from direct integration of (9b) with variable E_w (blue-solid line) panel (a). Time history of the carrier wave-number in the case of *S1* (black- cross line), and from analytic Equation (10), with β_g calculated in two fashions described just above constant E_w (blue-solid line) and variable E_w (red-solid line) panel (b).

wave-number is proportional to γ_g (see Eq. (10)), it is very sensitive to β_g variations as does γ_g itself. In Fig (6b), we have plotted the time history for carrier wave-number in the case of *S1* both from the simulations and the analysis. In the analytical case, we used formula (10) with β_g calculated in the two fashions described just above. It is observed that the including E_w-variations, noticeably

increases the accuracy of the analytical result at long times. All plotted curves, in Fig (6b), excellently merge at early times in the favor of Eq. (9b). Note that long-term match is not expected in this case, as it is already mentioned above that the validity of Eq. (10) is restricted to early times.

The deviation expectedly observed between Eq. (10) and simulations at long times, in Fig (6b), is attributed to the plasma wavelength lengthening originated from the wake amplification [21]. As already pointed out in Sec. III on Fig. 3, the plasma wave and the laser pulse propagate with the same phase velocity causing the laser wavelength to increase precisely according to the plasma wavelength lengthening.

C. THE ORIGIN AND THE INTERPRETATION OF THE ANOMALOUS GROUP VELOCITY BEHAVIORS

The origin of the obtained high group-velocities may be questioned concerning its anomaly respect to the commonly accepted result from the linear theory. The answerer is obscured in the essential difference between a fundamental plasma mode and its included electromagnetic fields. Generally, in a plasma mode, both electromagnetic fields and the plasma charges are included into a single physical entity which loses its meaning if either of these components be eliminated. Therefore, the individual group and phase velocities of the electromagnetic fields

do not necessarily coincide with that of the corresponding plasma mode. In the case of our problem, the linear group velocity corresponds to the transverse, electromagnetic plasma modes. Since the laser pulse alone is not identical to or a superposition of electromagnetic plasma modes, the deviation of pulse group velocity from the linear value is natural.

In fact, the linear group velocity is the asymptotic form of the *total (plasma+light) energy* transport rate, say v_{gt}, at very low intensities [37]. This rate is given by $v_{gt} = S_t / U_t$ where $S_t \equiv \int \mathrm{dx}[c^2 g_x + m_e c^2 \gamma_e n_e v_{ex}]$ and $U_t = \int \mathrm{dx}[u_{EM} + m_e c^2 \gamma_e n_e]$ are the total-energy flux and the total energy respectively [37]. It is very different from our group velocity (Eq. 8) which is the rate of radiation energy transport.

In order to better understand the above statements, consider the definition $v_{gt} = S_t / U_t$ in the linear regime, i.e. $v_{gt} = v_g^0 = k_0 / \omega_0$ [37]. In this case, the *commoving frame of the (light+plasma) disturbance*, we term as the *primed frame,* moves with velocity v_g^0. The pulse carrier-frequency and the carrier-wave-number respectively assume the values $\omega_0' = \omega_p$ and $k_0' = 0$ in the primed frame (prime indicate measurement in the primed frame). To be convinced about these relations, it may be noticed that using Lorentz transformations, these equations give

$\omega_0 = \gamma_g^0 \omega_p$ and $k_0 = \gamma_g^0 \beta_g^0 \omega_p / c$ in the laboratory frame where $\beta_g^0 = v_g^0 / c$ and $\gamma_g^0 = [1-(\beta_g^0)^2]^{-1/2}$. Dividing the obtained equation for ω_0, by the equation for k_0, we get $v_\phi^0 \equiv \omega_0 / k_0 = c^2 / v_g^0$, the well-known relation between the phase (v_ϕ^0) and group (v_g^0) velocities of the electromagnetic modes in the linear theory. Also, we can easily check that ω_0 and k_0 satisfy the linear dispersion relation, $\omega_L^2(k) = c^2 k^2 + \omega_p^2$. Since, the equation $\omega_0' = \omega_p$, contradicts the equation $[\omega_0 \approx 0]\big|_{PCM}$, used and described in relation with Eq. (10), our PCM frame is completely different from the primed frame and our group velocity (Eq. 8) should differ from the well-known linear value and its nonlinear correspondence, v_{gt}.

Based on contents of Sec. III and Sec. IV.B, our PCM frame is the electron plasma-wave phase frame on which the plasma does not perform temporal oscillations and variation. And since this frame is also the proper frame of radiation ($H_0 = \text{const}$, Eq. (7a)), our global pulse group velocity (Eq. (10) equals the averaged electron plasma-wave phase velocity. In this respect, Eq. (8) gains over the other group velocity expressions like $v_{gt} = S_t / U_t$, as, in applications, it is mostly desired to find a group velocity with the simplest relation with the electron plasma-wave phase velocity.

D. LOCAL DETAILS AND SPECTRAL ANALYSES

In the previous subsections, we have mainly described the *overall* pulse-evolutions by characterizing the global group velocity. However, the interaction shows noticeable local behaviors, as C_W-envelope, the effective potential of the radiation suggested by Eqs. (6) (see descriptions on Fig. 1), has a spatially variant gradient. Even more, the effective potential undergoes slow temporal evolutions according to the plasma-wave evolutions. As a result the pulse undergoes modulations both in its amplitude and in its phase, as briefly and qualitatively described on Fig. 1. The equality between the light and the plasma-wave phase velocities, described in Sec. III and Sec. IV.C, can help to simplify the problem, but, still, the full quantitative account of the spatiotemporal pulse evolutions, based on Eqs. (6), seems impossible. A part of this difficulty arises from nonexistence of a simple relation for the local phase velocity in terms of the local light energy (u_{EM}) and momentum (g_x) densities (see discussions concerning complexities in reducing tensors to vectors in Sec. 6 of Ref [49]).

At the adiabatic conditions, all local light (plasma-wave) phase velocities in the pulse region approximately equal the global group velocity (8), due to very slow variations in the plasma wave. This further simplifies the situation and even more simplification follows by considering the solution of the wave equation, $[\partial^2 / \partial x^2 - c^{-2}\partial^2 / \partial t^2]a_y = (\omega_p^2 / n_{e0})(n_e / \gamma_e)a_y$, in the PCM frame and in the Fourier

space instead of the real space. The simplifying fact is that, due to the approximately zero temporal evolutions of the plasma in the PCM frame, the coupling between the plasma wave and radiation, in the right hand side of the wave equation, produces only new wave-numbers and not new frequencies. This is consistent with the local conservation laws, Eqs (6), which state that while the local radiation momentum changes by wake-excitation, the radiation energy is totally conserved. Therefore, for a newly produced mode in the PCM frame, $(\omega,k)\big|_{PCM}$, we have $\omega\big|_{PCM}=\omega_0\big|_{PCM}$ and $k\big|_{PCM}=[k_0+\Delta k]\big|_{PCM}$. Here, Δk is the wave-number shift introduced by plasma, and, ω_0 and k_0 are the original (pump) frequency and wave number. Using Lorentz transformations for (ω,k) and noting these transformations for ω_0 and k_0 themselves, i.e. $\omega_0=\gamma_g(\omega_0\big|_{PCM}+\beta_g c\,k_0\big|_{PCM})$ and $k_0=\gamma_g(k_0\big|_{PCM}+\beta_g\,\omega_0\big|_{PCM}/c)$, we obtain,

$$k=k_0+\gamma_g\Delta k\big|_{PCM}. \tag{11a}$$

$$\omega=\omega_0+\gamma_g\,c\beta_g\Delta k\big|_{PCM}. \tag{11b}$$

These equations, generally predict spectral broadening already observed on Fig. 2.

The occurrence of the so-called electromagnetic-cascading can be predicted by Eqs.(11), in agreement with the recent observations [38, 47, 48]. In the case of flat-top pulses with lengths longer than the plasma wavelength, the excited plasma

wave is periodic inside the uniform part of the pulse. Therefore, the Fourier expansion of n_e / γ_e in the right hand side of the wave equation produces wave-numbers in multiples of the plasma-wave wave-number, i.e. $\Delta k_l\big|_{PCM} = \pm 2\pi l / \lambda_p^{NL}\big|_{PCM}$ with $l = 0,1,2,....$ In the other hand, the plasma wavelength undergoes the Fitzgerald contraction in the laboratory frame with respect to the PCM frame, i.e. $\lambda_p^{NL} = \lambda_p^{NL}\big|_{PCM} / \gamma_g$ and $\Delta k_l\big|_{PCM} = \pm 2\pi l / \gamma_g \lambda_p^{NL}$. Substituting this equation into (11a) and (11b), we obtain the following phase-relations between the *l*th mode and the pump mode, in the case of flat-top pulses with lengths longer than the plasma wavelength,

$$k_l = k_0 \pm 2\pi l / \lambda_p^{NL}. \tag{11c}$$

$$\omega_l = \omega_0 \pm 2\pi c \beta_g l / \lambda_p^{NL}. \tag{11d}$$

In order to examine Eqs. (11c) and (11d), for example in the case of *S2*, at $t = 0.54\text{ps}$ (corresponding to data plotted in Fig. (2b) in green color), the first two potential peaks (from the pulse front) are respectively located at $189\mu\text{m}$ and $175\mu\text{m}$, giving the estimation $\lambda_p^{NL} = 14\mu\text{m}$ for the plasma wavelength. Substituting this estimation into Eq. (11c), we obtain $k_l \approx k_0 \pm 0.075 k_0 l$. This result is in the good agreement with the data plotted in Fig. (2b), as, the distance between k_1 and k_2, pointed by two arrows in the figure, is 0.066.

As long as the pulse decelerations has not been fully developed, the group velocity is ultra-high ($\beta_g \approx 1$) and we have $\omega_0 \approx ck_0$ (see Eq. 10). Therefore Eqs (11a) and (11b) result in,

$$\omega = ck, \tag{11e}$$

i.e. the dispersion curve assumes the linear relation and the new modes appear as the vacuum electromagnetic modes in the laboratory. In Fig 7, we have plotted the dispersion relation at three different time instances for simulations *S1* (a-c), *S2* (d-f) and *S3* (g-i). In the case of *S1*, it is observed that dispersion curve exactly obeys the linear relation (11e) even at very long times. Note that the linear relation does not mean that the plasma dispersion acts in the same way as in the linear regime. Here, despite to the linear regime, the spectral-density undergoes very large evolutions along the dispersion curve. This phenomenon is the full nonlinear analogy of the displacement of the electromagnetic pump mode in the quasi-linear Raman scattering. In the case of *S2*, the agreement at early times is prefect but at long times the situation becomes doubtful at low *k* values. By using higher density values in the case of *S3*, clear deviation of dispersion from the linear relation at low *k* values is observed at long times, a phenomenon which is attributed to the violation of the adiabatic conditions.

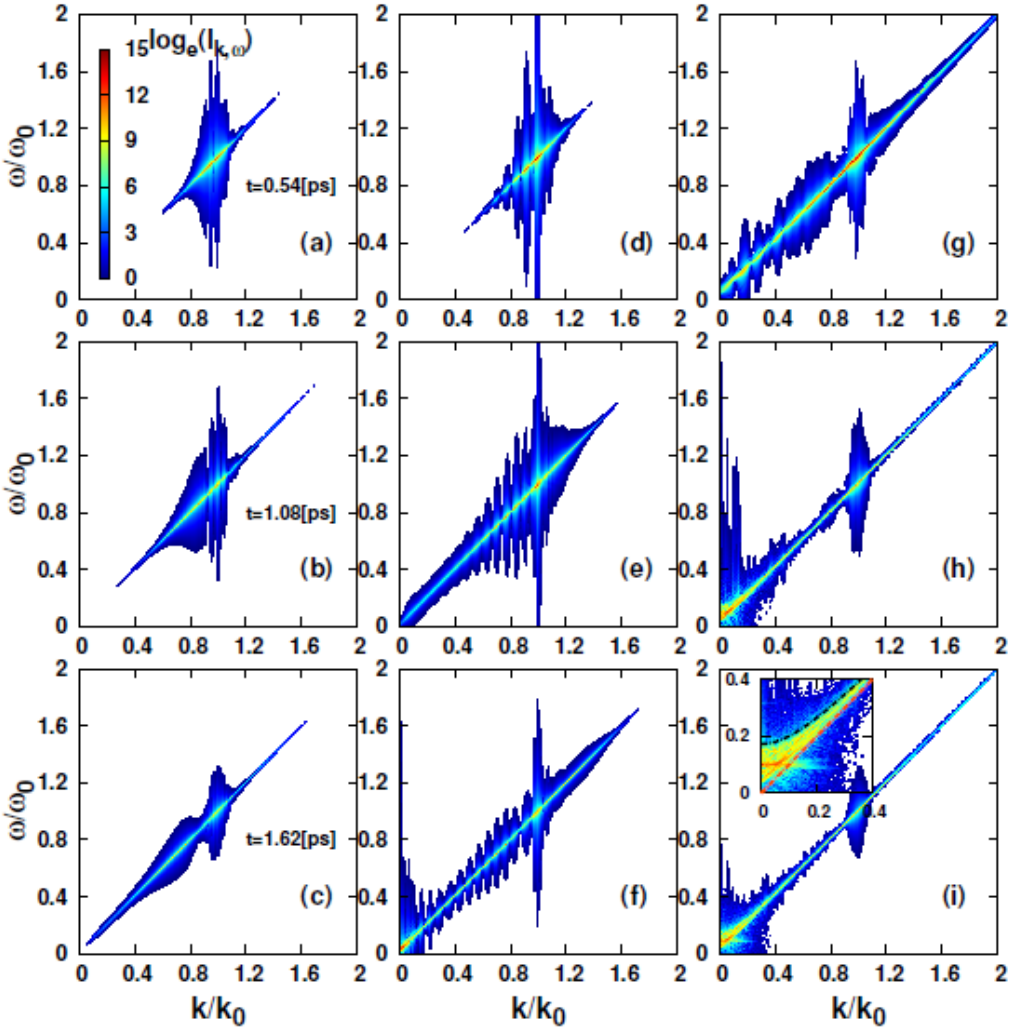

Fig. 7. (Color online): Dispersion relation at three different time instances t=0.54ps, t=1.08ps and t=1.62ps, for simulation cases *S1* panels (a-c), *S2* panels (d-f) and *S3* panels (g-i). In the onset of panel (i) the broken lines are the dispersion relations, $\omega = ck$ **(red) and** $\omega^2 = ck^2 + \omega_p^2$ **(black).**

V. RADIATION BACK-REACTIONS AND THE NON-ADIABATIC REGIME

The validity of our adiabatic description (elaborated in Sec. IV) necessitates very slow wakefield (C_w) evolutions in the PCM frame. The wakefield (C_w) evolutions can be considered as the radiation back-reaction to the plasma, as a

response to the imposed variations in the radiation energy-momentum. These evolutions are derived by the local radiation variations which themselves are proportional to the local force density, $E_p^2 \partial C_W / \partial x$ (Eq. (6b)). Therefore, the local rate of change in the wake excitation profile, C_w, also scales as a factor proportional to this force density. Obviously, the C_w-evolutions may be assumed slow only if the plasma, in the PCM frame, can leave any given location of the radiation evolutions such a fast that no in-place interaction could be established. At these conditions the wake excitation is exclusively attributed to the common ponderomotive force produce by the space variations of the instantaneous pulse profile and the adiabaticity is preserved. Therefore, in order to obtain a quantitative condition for adiabaticity, the force density, $E_p^2 \partial C_W / \partial x$, should be compared against the local plasma momentum density in the PCM frame. The amount of the momentum change by $E_p^2 \partial C_W / \partial x$ during the relevant scale time ω_p^{-1} is given by $\omega_p^{-1} E_p^2 \partial C_W / \partial x$. This amount should be very smaller than the local momentum density $[m_e c n_e \gamma_e \beta_{e.x}]\big|_{PCM}$. Therefore, the necessary condition for the adiabatic behavior reads as,

$$\frac{1}{\gamma_g \beta_g}\left[\frac{\partial C_W}{\gamma_e \partial x}\right]\Bigg|_{PCM} << \frac{\omega_p}{c} \qquad (12)$$

where we have used the continuity equation (3a) together with the relations $E_p = m_e c\omega_p / e$ and $\omega_p^2 = n_{e0}e^2 / \varepsilon_0 m_e$ for simplifying the result.

Base on Eq. (12), the wakfield evolves faster if the pulse deceleration results in low *local* group velocities (low $\gamma_g\beta_g$), if steep wake profiles are produced (high $\partial C_W / \partial x$) , for example, in a high density plasma and/or via the interaction of strong laser pulses, and if the local plasma gamma factor, γ_e, in the PCM frame reduces noticeably from γ_g. The last condition is typically occurred at minima of the electric potential and in the most violent case at wake amplitudes near the fluid wave break threshold [42, 44, 45]. And if sufficiently fast, the wakefield evolutions can result in violation of adiabaticity.

The wakefield evolutions appear in the forms of light phase and amplitude modulations. In agreement with the above analyses, the pulse modulation develops quickly at the density-maxima (potential minima) locations, as already noticed in Fig (1). Reminding our above discussions about the plasma wave phase-velocity, its evolution and its local equality with the light phase-velocity, it is now clear that the light modulation, observed to occur at the density peaks in Fig.1, is initiated by the phase-velocity modulations due to the plasma wavelength lengthening described in [21]. Then the modulation development is further and further accelerated by the resultant decrease in the local group velocity and increase in the

steepening. When the amplitude of the excited wake is initially larger (typically at higher densities), the evolution toward this situation is faster (compare Figs 3 and 4 for *S2* and *S3* respectively and note the corresponding wake-amplitude histories, Figs (5b) and (5c).

As long as the wakefield evolution does not induce non-slow phase modulations (highly local phase velocities), the spectrum evolution keep its adiabatic characters. To better understand this statement, see the assumptions made in deriving Eq. (10) and its following adiabatic equations. Due to the wakefield amplification (amplitude modulation) and whence plasma-wave steepening, the *k*-spectrum may extend further and further away from the central mode and toward the small values in the course of time (see Fig. 2a) but the dispersion keep the linear form Fig. 7(a-c). The mechanism of the extension is growth of $\Delta k\big|_{PCM}$-amplitude in the PCM frame due to the steepening resulting in lower-*k* modes in the laboratory frame (see Eq. 11a). On the other hand when noticeable phase modulations are encountered, the validity of the obtained results is limited to early times. For example it is observed in Figs. 2 and 7, that the electromagnetic cascading, outlined in Sec. IV.D in the case of $L_p > \lambda_{\mathrm{p}}^{\mathrm{NL}}$ (*S2, S4*), disappears at long times.

Phase-velocity modulations (phase-modulation), in the case of $L_p > \lambda_{\mathrm{p}}^{\mathrm{NL}}$ (*S2-S4*), can cause to produce much lower *k*-modes and to introduce other new effects into the light spectrum. Since, near the adiabatic regime, the local light phase velocity equals the local plasma phase velocity, the reduction of the local plasma phase velocity can be modeled by doing the replacement $\{\beta_g, \gamma_g\} \to \{\beta_{ph.l}, \gamma_{ph.l}\}$ in Eqs. (10), (11a) and (11b). Here the subscript *ph.l* stands for the local plasma phase velocity. The resultant local form of Eq. (11a) obtained by this replacement, predicts wave-numbers reduced by amount $\gamma_{ph.l} / \gamma_g$ in the laboratory, in the presence of phase deceleration. In addition, a multi-hump structure is expected to appear in the spectrum due to noticeable decreases in $\gamma_{ph.l}$ at density peaks (quasi-discrete values in $\gamma_{ph.l}$). This structure is already observed in Figs. 2 (*S2-S4*) and 7 (*S2-S3*), i.e. a new local maxima is gradually developed around *k=0* and due to the noticeable decrease in $\gamma_{ph.l}$ at the density peak inside the laser pulse.

When either phase modulation is strong, in the sense that multi-hump structure is appeared, or amplitude modulation is fast, the energy conservation in the PCM, Eq. (6b), breaks down and the adiabatic analysis loses its validity. Especially, in the case of phase modulation plasma wave and the laser light become dephased. At these conditions, new frequencies, as well as new wave-numbers, are produce in the PCM frame via coupling of the radiation and the plasma in the right hand side

of the wave equation. Since, now, the dispersion relation is not linear, the dispersion plot undergoes $\omega-$space broadening as well as *k*-space broadening. This phenomenon is already observed in the dispersion plots Figs (7f-7i), and more clearly at low *k*-modes. When the wake excitation is saturated in the case of *S3*, the dispersion curve tends to the well known electromagnetic dispersion (see Fig. 7i).

VI. CONCLUSION

In conclusion, we have presented a detailed description of the intense, short laser pulse propagation through the under-dense plasma. Both the adiabatic and non adiabatic regimes have been considered for pulse lengths both larger and shorter than the plasma wavelength. We have shed light on the complex phenomena of pulse deceleration, pulse modulation and the transition from the stationary propagation into a semi-chaotic phase typically observed at high densities. For the first time, a proper modeling has been presented and formulated for the adiabatic regime. In this way, an analytic result has been obtained for the pulse group velocity (Eqs. (9b) and (9c)), being equal to the averaged plasma-wave phase-velocity in the pulse region, and the anomalous behaviors of the result have been fully discussed. The necessary condition for the quasi-stationary propagation of the intense pulse has been obtained (Eq. (12) and its connection with the pulse

modulation has been described. Finely, the anomalous nature of the plasma dispersion in the full nonlinear regime has been outlined and has been discussed in relation with the observed novel phenomena.

REFERENCE

[1] Strickland D and Mourou G 1985 *Opt. Commun* **56** 447

[2] Mourou G, Barty C P J and Perry M D 1998 *Phys. Today.* **51** 22

[3] Santala M I K *et al* 2000 *Phys.Rev.Lett.* **84** 1459

[4] Malka V *et al* 2002 *Science* **298** 1596

[5] Mangles S P D *et al* 2004 *Nature* **431** 535

[6] Geddes C G R, Toth C, van Tilborg J, Esarey E, Schroeder C B, Bruhwilder D, Nieter C, Cary J and Leemans W P 2004 *Nature* **431** 538

[7] Leemans W P, Nagler B, Gonsalves A J, Toth Cs, Nakamura K, Geddes G G R, Esarey E, Schroeder C B and Hooker S M 2006 *Nature. Phys.* **2** 696

[8] Li Y T *et al* 2004 *Phys. Rev. E* **69** 036405

[9] Willingale L *et al* 2006 *Phys. Rev. Lett.* **96** 245002

[10] Willingale L *et al* 2009 *Phys. Rev. Lett.* **102** 125002

[11] Faure J, Glinec Y, Pukhov A, Kiselev S, Gordienko S, Lefebvre E, Rousseau J P, Burgy F and Malka V 2004 *Nature* **431** 541

[12] Rousse A *et al* 2003 *Phys. Rev. Lett.* **93**, 135005 (2003).

[13] Tabak M, Hammer J, Glinsky M E, Kruer W L, Wilks S C, Woodworth J, Campbell E M, Perry M D and Mason R J 1994 *Phys. Plasmas* **1** 1626

[14] Bulanov S V, Inovenkov I N, Kirsanov V I, Naumova N M and Sakharov A S 1992 *Phys. Fluids B* **4** 1935

[15] Decker C D, Mori W B, Tzeng K C and Katsouleas T 1996 *Phys. Plasmas* **3** 2047

[16] Mori W B 1997 *IEEE Journal of Quantum Electronics* **33** 1942

[17] Ren C, Duda B J, Hemker R G, Mori W B, Katsouleas T, Antonsen, Jr. T M and Mora P 2001 *Phys. Rev. E* **6**3 026411

[18] Gordon D F, Hafizi B, Hubbard R F, Pen˜ano J R, Sprangle P and Ting A 2003 *PRL* **90** 215001

[19] Faure J, Glinec Y, Santos J J, Ewald F, Rousseau J P, Kiselev S, Pukhov A, Hosokai T and Malka V 2005 *PRL* **95** 205003

[20] Shadwick B A, Schroeder C B and Esarey E 2009 *Physics of Plasmas* **16** 056704

[21] Schroeder C B, Benedetti C, Esarey E and Leemans W P 2011 *PRL* **106** 135002

[22] Bu Z and Ji P 2012 *Phys. Plasmas* **19** 113114

[23] Benedetti C, Rossi F, Schroeder C B, Esarey E and Leemans W P 2015 *Phys. Rev. E* **92** 023109

[24] Sheng Z M, Mima K, Zhang J and Meyer-ter-Vehn J 2004 *Phys. Rev. E* **69** 016407

[25] Sgattoni A, Londrillo P, Macchi A and Passoni M 2012 *Phys. Rev. E* **85** 036405

[26] Sylla F, Flacco A, Kahaly S, Veltcheva M, Lifschitz A, Malka V, d'Humières E, Andriyash I and Tikhonchuk V 2013 *Phys. Rev. Lett.* **110** 085001

[27] Passoni M *et al* 2014 *Plasma Phys. Control. Fusion* **56** 045001

[28] Yazdani E, Sadighi-Bonabi R, Afarideh H, Yadanpanah J, Hora H 2014 *Laser Part. Beam*s **32** 509

[29] Bochkarev S G, Brantov A V, Bychenkov V Yu, Torshin D V, Kovalev V F, Baidin G V, Lykov V A 2014 *Phys. Rep*. **40** 202

[30] Bin J H *et al* 2015 *Phys. Rev. Lett.* **115** 064801

[31] khalilzadeh E, Yazdanpanah J, Jahanpanah J, chakhmachi A and Yazdani E 2015 *Phys. Plasmas* **22** 113115

[32] Antonsen, Jr. T M and Mora P 1992 *Phys. Rev. Lett.* **69** 2204

[33] Sakharof A S and Kirsanov V I 1994 *Phys. Rev. E* **49** 3274

[34] Mori W B, Decker C D, Hinkel D E and Katsouleas T 1994 *Phys. Rev. Lett.* **72** 1482

[35] Barr H C, Mason P and Parr D M 1999 *Phys. Rev. Lett.* **83** 1606

[36] Quesnel B, Mora P, Adam J C, Guérin S, Héron A and Laval G 1997 *Phys. Rev. Lett*. **78** 2132

[37] Decker C D and Mori W B 1994 *Phys. Rev. Lett*. **72** 490

[38] Moore C I, Ting A, Krushelnick K, Esarey E, Hubbard R F, Hafizi B, Burris H R, Manka C and Sprangle P 1997 *Phys. Rev. Lett.* **79** 3909

[39] Krall J, Ting A, Esarey E and Sprangle P 1993 *Phy. Rev. E* **48** 215

[40] See supplemental material A [Here, it is shown that the set of equations (1) can result the covariant conservations laws of equations (2)].

[41] Tajima T and Dawson J M 1979 *Phys. Rev. Lett*. **43** 267

[42] Sprangle P, Esarey E and Ting A 2004 *Phys. Rev. A* **4**1 4463

[43] Yazdanpanah J and Anvary A 2009 *Phys. Plasmas* **16**, 023104

[44] Yazdanpanah J and Anvary A 2014 *Phys. Plasmas* **21** 023101

[45] Schroeder C B and Esarey E 2010 *Phys. Rev. E* **81** 056403

[46] See supplemental material B [Here, it is explicitly shown that the common QSA equations could be obtained by assuming the time-independency in the *real Lorentz boost* PCM-frame and then transforming the reduced equations into the laboratory].

[47] Karttunen S J and Salomaa R R E 1986 *Phy. Rev. Lett* **56** 604

[48] Tzeng K C, Mori W B and Katsouleas T 1999 *Phys. Plasmas* **6** 2105

[49] Weinberg S 1972 *Gravitation and Cosmology: Principles and applications of general theory of relativity* John Wiley & Sons New York